Conservativity of Symplectic Methods for the Ablowitz-Ladik Discrete Nonlinear Schrödinger Equation*

Xiangtao Liu[1], Yuanchang Sun[1,2] & Yifa Tang[1†]

[1]LSEC, ICMSEC
Academy of Mathematics & Systems Science
Chinese Academy of Sciences
P.O. Box 2719, Beijing 100080, P.R. China

[2]Graduate School of the Chinese Academy of Sciences
Beijing 100080, P.R. China

Abstract

Using several kinds of Darboux transformations, we standardize the non-canonical symplectic structure of Ablowitz-Ladik model (**A-L model**) of the Nonlinear Schrödinger Equation (**NLSE**), then we employ some symplectic schemes to simulate the solitons motion and test the evolution of the discrete invariants of the **A-L model** and also the conserved quantities of the original **NLSE**. In comparison with the non-symplectic scheme applied directly to the **A-L model**, we show the overwhelming superiorities of the symplectic methods. We also compare the numerical results and implementation processes of same symplectic schemes applied to different standardized Hamiltonian systems via different Darboux transformations, and show that with more complicated implementation process, the symmetric Darboux transformation improves the numerical results obtained via asymmetric one, in preserving the invariants of the **A-L model** and the original **NLSE**.

Key words: *Nonlinear Schrödinger Equation, Ablowitz-Ladik Model, Darboux transformation, symplectic methods, Invariants.*

*This research is supported by the *Informatization Construction of Knowledge Innovation* Projects of the Chinese Academy of Sciences *"Supercomputing Environment Construction and Application"* (INF105-SCE), and by a grant (No. 10471145) from National Natural Science Foundation of China, and by Morningside Center of Mathematics, Chinese Academy of Sciences.

†Corresponding author. E-mail: tyf@lsec.cc.ac.cn

1 Introduction

We consider the nonlinear cubic Schrödinger Equation (**NLSE**) with initial condition

$$\begin{cases} iW_t + W_{xx} + a|W|^2W = 0, \\ W(x,0) = W_0(x) \end{cases} \tag{1}$$

where $x \in \mathbb{R}$, $a > 0$ is a constant and $W(x,t)$ is a complex function. Different initial conditions $W_0(x)$ decide different motions. For example, some kind of $W_0(x)$ with $W_0(\pm\infty) = 0$ will produce bright solitons motion (see [5, 10]). It is known that **NLSE** (1) has an infinite number of conserved quantities such as the *charge*, the *momentum*, the *energy*, $\cdots$. We write the first six as follows (refer to Zakharov & Shabat [17]):

$$\begin{aligned}
F_1 &= \int_{-\infty}^{+\infty} |W|^2 dx, \\
F_2 &= \int_{-\infty}^{+\infty} \left\{ W\frac{d\overline{W}}{dx} - \overline{W}\frac{dW}{dx} \right\} dx, \\
F_3 &= \int_{-\infty}^{+\infty} \left\{ 2\Big|\frac{dW}{dx}\Big|^2 - a|W|^4 \right\} dx, \\
F_4 &= \int_{-\infty}^{+\infty} \left\{ 2\frac{d\overline{W}}{dx}\frac{d^2W}{dx^2} - 3a|W|^2\overline{W}\frac{dW}{dx} \right\} dx, \\
F_5 &= \int_{-\infty}^{+\infty} \left\{ 2\Big|\frac{d^2W}{dx^2}\Big|^2 - 6a|W|^2\Big|\frac{dW}{dx}\Big|^2 - a\Big(\frac{d|W|^2}{dx}\Big)^2 + a^2|W|^6 \right\} dx, \\
F_6 &= \int_{-\infty}^{+\infty} \left\{ 2\frac{d^2\overline{W}}{dx^2}\frac{d^3W}{dx^3} - 5a\Big|\frac{dW}{dx}\Big|^2\frac{d|W|^2}{dx} - 10a|W|^2\frac{d\overline{W}}{dx}\frac{d^2W}{dx^2} + 5a^2|W|^4\overline{W}\frac{dW}{dx} \right\} dx
\end{aligned}$$

where $\overline{W}$ is the complex conjugation of W.

For equation (1), one popular spatial discretization model is

$$i\frac{dW_l}{dt} + \frac{W_{l+1} - 2W_l + W_{l-1}}{h^2} + \frac{a}{2}|W_l|^2(W_{l+1} + W_{l-1}) = 0\,, \tag{2}$$

where h is the spatial step-size and $W_l(t) = W(lh,t)$, $l = \cdots, -1, 0, 1, \cdots$. This discrete model is the well-known Ablowitz-Ladik Model (**A-L model**). It is proven that the solution of **A-L model** (2) converges to that of the original continuous **NLSE** (1) when $h \longrightarrow 0$ (see [15]). (2) is a completely integrable system (see [1, 5, 8, 10]), but it has a noncanonical symplectic structure for which standard symplectic integrators are not applicable. Via generating functions technique (see [9, 13]) or standardization of the noncanonical symplectic structure (see [15, 16]), people have already constructed symplectic numerical methods for the **A-L model** (2).

In this paper, we give an easy program for calculation of the first six discrete invariants of the **A-L model** (section 2), and construct approximations of the first six conserved quantities of the original **NLSE** by using centered differences (section 3), then provide three kinds of Darboux transformations to standardize the **A-L model**

(section 4), and then use two symplectic schemes to simulate the solitons motion and test the evolution of the discrete invariants of the **A-L model** and also the conserved quantities of the original **NLSE**, for two different standardized hamiltonians, in comparison with a non-symplectic method applied directly to the **A-L model** (section 5-6), finally give some concluding remarks in section 7.

2 Discrete Invariants of Ablowitz-Ladik Model

With the transformations $X_l = \sqrt{\frac{ah^2}{2}} W_l$, $l = \cdots, -1, 0, 1, \cdots$; $s = -\frac{1}{h^2}t$, we change (2) into

$$i\frac{dX_l}{ds} = X_{l+1} - 2X_l + X_{l-1} + |X_l|^2(X_{l+1} + X_{l-1}) = 0. \tag{3}$$

(3) is a typical nonlinear differential-difference equation, it possesses an infinite number of conservation laws of motion C_m ($\frac{dC_m}{ds} = 0$). Following Zakharov and Shabat [17], these laws can be constructed systematically from a scattering problem by considering asymptotic expansions (refer to Ablowitz & Ladik [1]).

Using some intermediate quantities $g_k^{(j)}$ ($j = 1, \cdots, 6$; $k = \cdots, -1, 0, 1, \cdots$) (as introduced in [1]), we give some program for fast calculation of C_m ($m = 1, \cdots, 6$) in a recursive manner:

$$\begin{aligned}
-\overline{X}_k &= \frac{g_{k+2}^{(1)}}{X_{k+1}}, \\
0 &= \frac{g_{k+2}^{(2)}}{X_{k+1}} + X_k\frac{g_{k+1}^{(1)}}{X_k}\frac{g_{k+2}^{(1)}}{X_{k+1}} - \frac{g_{k+1}^{(1)}}{X_k}, \\
0 &= \frac{g_{k+2}^{(3)}}{X_{k+1}} + X_k\frac{g_{k+1}^{(1)}}{X_k}\frac{g_{k+2}^{(2)}}{X_{k+1}} + X_k\frac{g_{k+1}^{(2)}}{X_k}\frac{g_{k+2}^{(1)}}{X_{k+1}} - \frac{g_{k+1}^{(2)}}{X_k}, \\
0 &= \frac{g_{k+2}^{(4)}}{X_{k+1}} + X_k\frac{g_{k+1}^{(1)}}{X_k}\frac{g_{k+2}^{(3)}}{X_{k+1}} + X_k\frac{g_{k+1}^{(2)}}{X_k}\frac{g_{k+2}^{(2)}}{X_{k+1}} + X_k\frac{g_{k+1}^{(3)}}{X_k}\frac{g_{k+2}^{(1)}}{X_{k+1}} - \frac{g_{k+1}^{(3)}}{X_k}, \\
0 &= \frac{g_{k+2}^{(5)}}{X_{k+1}} + X_k\frac{g_{k+1}^{(1)}}{X_k}\frac{g_{k+2}^{(4)}}{X_{k+1}} + X_k\frac{g_{k+1}^{(2)}}{X_k}\frac{g_{k+2}^{(3)}}{X_{k+1}} + X_k\frac{g_{k+1}^{(3)}}{X_k}\frac{g_{k+2}^{(2)}}{X_{k+1}} \\
&\quad + X_k\frac{g_{k+1}^{(4)}}{X_k}\frac{g_{k+2}^{(1)}}{X_{k+1}} - \frac{g_{k+1}^{(4)}}{X_k}, \\
0 &= \frac{g_{k+2}^{(6)}}{X_{k+1}} + X_k\frac{g_{k+1}^{(1)}}{X_k}\frac{g_{k+2}^{(5)}}{X_{k+1}} + X_k\frac{g_{k+1}^{(2)}}{X_k}\frac{g_{k+2}^{(4)}}{X_{k+1}} + X_k\frac{g_{k+1}^{(3)}}{X_k}\frac{g_{k+2}^{(3)}}{X_{k+1}} \\
&\quad + X_k\frac{g_{k+1}^{(4)}}{X_k}\frac{g_{k+2}^{(2)}}{X_{k+1}} + X_k\frac{g_{k+1}^{(5)}}{X_k}\frac{g_{k+2}^{(1)}}{X_{k+1}} - \frac{g_{k+1}^{(5)}}{X_k}.
\end{aligned}$$

$$C_1 = \sum_k g_k^{(1)},$$

$$
\begin{aligned}
C_2 &= \sum_k \Big\{ g_k^{(2)} - \frac{1}{2}[g_k^{(1)}]^2 \Big\}, \\
C_3 &= \sum_k \Big\{ g_k^{(3)} - g_k^{(2)} g_k^{(1)} + \frac{1}{3}[g_k^{(1)}]^3 \Big\}, \\
C_4 &= \sum_k \Big\{ g_k^{(4)} - g_k^{(3)} g_k^{(1)} - \frac{1}{2}[g_k^{(2)}]^2 + g_k^{(2)}[g_k^{(1)}]^2 - \frac{1}{4}[g_k^{(1)}]^4 \Big\}, \\
C_5 &= \sum_k \Big\{ g_k^{(5)} - g_k^{(4)} g_k^{(1)} - g_k^{(3)} g_k^{(2)} + g_k^{(3)}[g_k^{(1)}]^2 + [g_k^{(2)}]^2 g_k^{(1)} \\
&\qquad -g_k^{(2)}[g_k^{(1)}]^3 + \frac{1}{5}[g_k^{(1)}]^5 \Big\}, \\
C_6 &= \sum_k \Big\{ g_k^{(6)} - g_k^{(5)} g_k^{(1)} - g_k^{(4)} g_k^{(2)} + g_k^{(4)}[g_k^{(1)}]^2 - \frac{1}{2}[g_k^3]^2 + 2 g_k^{(3)} g_k^{(2)} g_k^{(1)} \\
&\qquad -g_k^{(3)}[g_k^{(1)}]^3 + \frac{1}{3}[g_k^{(2)}]^3 - \frac{3}{2}[g_k^{(2)}]^2[g_k^{(1)}]^2 + g_k^{(2)}[g_k^{(1)}]^4 - \frac{1}{6}[g_k^{(1)}]^6 \Big\}.
\end{aligned}
$$

Correspondingly, we will write out the expansions of the invariants of the **A-L model** (2): S_m ($S_m = -\frac{2}{ah^2} C_m$), $1 \le m \le 6$ in the Appendix. And we will test the evolution of $E_m = ER_m + iEI_m$ (ER_m and EI_m are the real part and imaginary part of E_m respectively, and $E_m = -\frac{2}{ah} C_m$), $1 \le m \le 6$ during numerical simulations in Section 6.

3 Approximations of conserved quantities of NLSE

Utilizing centered difference

$$
\begin{aligned}
W_x(lh,t) &= \frac{W_{l+1} - W_{l-1}}{2h}, \\
W_{xx}(lh,t) &= \frac{W_{l+1} - 2W_l + W_{l-1}}{h^2}, \\
W_{xxx}(lh,t) &= \frac{W_{l+2} - 2W_{l+1} + 2W_{l-1} - W_{l-2}}{2h^3},
\end{aligned}
$$

we can approximate the conserved quantities $F_1, \cdots, F_6$ of the original NLSE (1) as follows:

$$
\begin{aligned}
\widetilde{F}_1 &= h \sum_l W_l \overline{W}_l, \\
\widetilde{F}_2 &= \sum_l \left\{ W_l \overline{W}_{l+1} - W_{l+1} \overline{W}_l \right\}, \\
\widetilde{F}_3 &= \frac{1}{2h} \sum_l \left\{ 2|W_l|^2 - W_{l+1}\overline{W}_{l-1} - W_{l-1}\overline{W}_{l+1} \right\} - ah \sum_l |W_l|^4, \\
\widetilde{F}_4 &= \frac{1}{h^2} \sum_l \left\{ 2W_{l+1}\overline{W}_l - 2W_l\overline{W}_{l+1} - W_{l+1}\overline{W}_{l-1} + W_{l-1}\overline{W}_{l+1} \right\} \\
&\quad -\frac{3a}{2} \sum_l |W_l|^2 \overline{W}_l \left\{ W_{l+1} - W_{l-1} \right\},
\end{aligned}
$$

$$
\begin{aligned}
\widetilde{F}_5 &= \frac{2}{h^3}\sum_l \left\{6|W_l|^2 - 4W_{l+1}\overline{W}_l - 4W_l\overline{W}_{l+1} + W_{l+1}\overline{W}_{l-1} + W_{l-1}\overline{W}_{l+1}\right\} \\
&\quad -\frac{3a}{2h}\sum_l |W_l|^2\left\{2|W_{l+1}|^2 - W_{l+1}\overline{W}_{l-1} - W_{l-1}\overline{W}_{l+1}\right\} \\
&\quad -\frac{a}{2h}\sum_l \left\{|W_l|^4 - |W_{l+1}|^2|W_{l-1}|^2\right\} + a^2h\sum_l |W_l|^6, \\
\widetilde{F}_6 &= \frac{1}{h^4}\sum_l \left\{5W_{l+1}\overline{W}_l - 5W_l\overline{W}_{l+1} - 4W_{l+1}\overline{W}_{l-1} + 4W_{l-1}\overline{W}_{l+1}\right. \\
&\qquad \left. +W_{l+2}\overline{W}_{l-1} - W_{l-1}\overline{W}_{l+2}\right\} \\
&\quad +\frac{5a}{8h^2}\sum_l \left\{|W_{l+1}|^2 - |W_{l-1}|^2\right\}\left\{W_{l+1}\overline{W}_{l-1} + W_{l-1}\overline{W}_{l+1}\right\} \\
&\quad +\frac{5a}{h^2}\sum_l |W_l|^2\left\{2W_l\overline{W}_{l+1} - 2W_l\overline{W}_{l-1} + W_{l+1}\overline{W}_{l-1} - W_{l-1}\overline{W}_{l+1}\right\} \\
&\quad +\frac{5a^2}{2}\sum_l |W_l|^4\overline{W}_l\left\{W_{l+1} - W_{l-1}\right\}.
\end{aligned}
$$

We will test the evolution of $\widetilde{F}_m = FR_m + iFI_m$ (FR_m and FI_m are the real part and imaginary part of $\widetilde{F}_m$ respectively), $1 \le m \le 6$ during numerical simulations in Section 6.

4 Standardization of the A-L model

With transformations $W_l = V_l \exp(-\frac{2ti}{h^2})$ and denotation $V_l = p_l + iq_l$, $l = \cdots, -1, 0, 1, \cdots$, we rewrite (2) as

$$
i\frac{dV_l}{dt} = -(\frac{1}{h^2} + \frac{a}{2}|V_l|^2)(V_{l+1} + V_{l-1}) \tag{4}
$$

or the following general Hamiltonian system

$$
\frac{d}{dt}Z = K^{-1}(Z)\nabla H(Z) \tag{5}
$$

where $Z = [p^\top, q^\top]^\top$, and $p = [p_{-n}, \cdots, p_n]^\top, q = [q_{-n}, \cdots, q_n]^\top$;

$$
K^{-1}(Z) = (k_{ij}(Z))_{(4n+2)\times(4n+2)} = \begin{bmatrix} O_{2n+1} & -D \\ D & O_{2n+1} \end{bmatrix} \tag{6}
$$

is anti-symmetric, nondegenerate and satisfies

$$
\frac{\partial k_{ab}(Z)}{\partial z_c} + \frac{\partial k_{bc}(Z)}{\partial z_a} + \frac{\partial k_{ca}(Z)}{\partial z_b} = 0, \quad a, b, c = 1, \cdots, 4n+2,
$$

$D = \mathrm{diag}\{U_{-n}, \cdots, U_n\}$, $U_l = 1 + \frac{ah^2}{2}(p_l^2 + q_l^2)$, $l = -n, \cdots, n$, O_{2n+1} is $(2n+1)\times(2n+1)$ null matrix; and

$$
H(Z) = \frac{1}{h^2}\sum_{l=-n}^{n}\left[p_l p_{l+1} + q_l q_{l+1}\right]. \tag{7}
$$

In the context of the Darboux theorem (see [2], [3]), (5) can be standardized. In fact for any general Hamiltonian system of the form (5), any transformation $\varphi : \mathbb{R}^{4n+2} \to \mathbb{R}^{4n+2}$, $\varphi(Y) = Z$ satisfying

$$\left[\frac{\partial \varphi}{\partial Y}\right]^{\top} K(\varphi(Y)) \left[\frac{\partial \varphi}{\partial Y}\right] = J \tag{8}$$

leads to a standard Hamiltonian system

$$\frac{d}{dt} Y = J^{-1} \nabla G(Y) \tag{9}$$

with $G(Y) = H \circ \varphi(Y)$, where $Y = [u^{\top}, v^{\top}]^{\top}$, $u = [u_{-n}, \cdots, u_n]^{\top}$, $v = [v_{-n}, \cdots, v_n]^{\top}$, $J = \begin{bmatrix} O_{2n+1} & I_{2n+1} \\ -I_{2n+1} & O_{2n+1} \end{bmatrix}$, I_{2n+1} is $(2n+1) \times (2n+1)$ identity matrix.

We note that in (6), $K^{-1}(Z)$ is completely splitable and so is $K(Z)$. Such being the special case, we can split the system in (8) into

$$\frac{\partial p_l}{\partial u_l} \frac{\partial q_l}{\partial v_l} - \frac{\partial q_l}{\partial u_l} \frac{\partial p_l}{\partial v_l} = U_l, \quad l = -n, \cdots, n. \tag{10}$$

Now it becomes easy to find a Darboux transformation by solving equations in (10). We list several solutions ([16]) as follows ($\lambda = \frac{ah^2}{2}$).

Darboux transformation **I**:

$$\begin{cases} p_l = \sqrt{\dfrac{1+\lambda v_l^2}{\lambda}} \tan\Big(\sqrt{\lambda\big(1+\lambda v_l^2\big)} u_l\Big), \\ q_l = v_l, \quad l = -n, \cdots, n \end{cases} \tag{11}$$

with inverse

$$\begin{cases} u_l = \dfrac{\arctan\left(\sqrt{\frac{\lambda}{1+\lambda q_l^2}} p_l\right)}{\sqrt{\lambda(1+\lambda q_l^2)}}, \\ v_l = q_l, \quad l = -n, \cdots, n \end{cases} \tag{12}$$

and standard Hamiltonian

$$\begin{aligned} G(u,v) = \frac{1}{h^2} \sum_{l=-n}^{n} \Bigg\{ & \sqrt{\frac{1+\lambda v_l^2}{\lambda}} \sqrt{\frac{1+\lambda v_{l+1}^2}{\lambda}} \tan\Big(\sqrt{\lambda\big(1+\lambda v_l^2\big)} u_l\Big) \\ & \tan\Big(\sqrt{\lambda\big(1+\lambda v_{l+1}^2\big)} u_{l+1}\Big) + v_l v_{l+1} \Bigg\}. \end{aligned} \tag{13}$$

Darboux transformation **II**:

$$\begin{cases} p_l = \sqrt{\dfrac{\exp\left(\lambda\{u_l^2 + v_l^2\}\right) - 1}{\lambda(u_l^2 + v_l^2)}} u_l, \\ q_l = \sqrt{\dfrac{\exp\left(\lambda\{u_l^2 + v_l^2\}\right) - 1}{\lambda(u_l^2 + v_l^2)}} v_l, \quad l = -n, \cdots, n \end{cases} \tag{14}$$

with inverse

$$\begin{cases} u_l = \sqrt{\dfrac{\ln\left(1+\lambda\{p_l^2+q_l^2\}\right)}{\lambda(p_l^2+q_l^2)}}\,p_l, \\ v_l = \sqrt{\dfrac{\ln\left(1+\lambda\{p_l^2+q_l^2\}\right)}{\lambda(p_l^2+q_l^2)}}\,q_l, \quad l=-n,\cdots,n \end{cases} \tag{15}$$

and standard Hamiltonian

$$G(u,v) = \frac{1}{h^2}\sum_l \left\{ \sqrt{\frac{\exp\left(\lambda\{u_l^2+v_l^2\}\right)-1}{\lambda(u_l^2+v_l^2)}} \sqrt{\frac{\exp\left(\lambda\{u_{l+1}^2+v_{l+1}^2\}\right)-1}{\lambda(u_{l+1}^2+v_{l+1}^2)}} \right. \left. [u_l u_{l+1}+v_l v_l] \right\}. \tag{16}$$

Darboux transformation **III**:

$$\begin{cases} p_l = \sqrt{\dfrac{\exp u_l - 1}{\lambda}}\cos(2\lambda v_l), \\ q_l = \sqrt{\dfrac{\exp u_l - 1}{\lambda}}\sin(2\lambda v_l), \quad l=-n,\cdots,n \end{cases} \tag{17}$$

with inverse

$$\begin{cases} u_l = \ln\Big(1+\lambda\big\{p_l^2+q_l^2\big\}\Big), \\ v_l = \dfrac{1}{2\lambda}\arctan\dfrac{q_l}{p_l}, \quad l=-n,\cdots,n \end{cases} \tag{18}$$

and standard Hamiltonian

$$G(u,v) = \frac{1}{\lambda h^2}\sum_{l=-n}^{n}\sqrt{(\exp u_l - 1)(\exp u_{l+1}-1)}\cos\left(2\lambda[v_l - v_{i+1}]\right). \tag{19}$$

Darboux transformation **I** has been successfully used to deal with the **A-L model** by Tang, Pérez-García and Vázquez [15]. They simulated the solitons motion and tested the evolution of the first three discrete invariants of the **A-L model**. As suggested by Hairer, Lubich and Wanner [7], Darboux transformation **II** treats the variables more symmetrically. This symmetry may improve the numerical results obtained by using Darboux transformation **I**. Darboux transformation **III** may bring some difficulty to numerical simulation, due to the illness of v_l depending on p_l in (18) and the derivatives of G with respect to u_l in (19), $l=-n,\cdots,n$.

5 Symplectic and nonsymplectic schemes

Since the **A-L model** (2) has already been changed into a standard Hamiltonian system, we can use the usual symplectic schemes (see [4, 6, 7, 12] for an introduction to symplectic numerical methods for Hamiltonian dynamics) straightforward. In comparison with the symplectic methods, we will also use a nonsymplectic scheme directly to the **A-L model**.

Scheme 1 (S1): the midpoint rule

$$\widetilde{Z} = Z + \tau f\Big(\frac{\widetilde{Z}+Z}{2}\Big) \tag{20}$$

where τ is the temporal step-size. The scheme **S1** is of 2nd order, revertible in τ. And it is symplectic for standard Hamiltonian systems ($f = J^{-1}\nabla H$), and preserves any quadratic invariant $Z^T S Z$ of the Hamiltonian H because

$$\begin{aligned}
\widetilde{Z}^T S\widetilde{Z} &= \widetilde{Z}^T S\Big[Z + \tau J^{-1}\nabla H\Big(\frac{\widetilde{Z}+Z}{2}\Big)\Big] \\
&= \widetilde{Z}^T SZ + (\widetilde{Z}+Z)^T S\tau J^{-1}\nabla H\Big(\frac{\widetilde{Z}+Z}{2}\Big) - Z^T S\Big[\tau J^{-1}\nabla H\Big(\frac{\widetilde{Z}+Z}{2}\Big)\Big] \\
&= Z^T SZ + \Big[\tau J^{-1}\nabla H\Big(\frac{\widetilde{Z}+Z}{2}\Big)\Big]^T SZ - Z^T S\Big[\tau J^{-1}\nabla H\Big(\frac{\widetilde{Z}+Z}{2}\Big)\Big] \\
&= Z^T SZ\,.
\end{aligned}$$

Scheme 2 (S2): third order scheme

$$\begin{cases}
\widetilde{Z} = Z + \dfrac{\tau}{2}[f(K_1) + f(K_2)]\,, \\
K_1 = Z + \dfrac{\tau}{6}\Big[3f(K_1) - \sqrt{3}f(K_2)\Big]\,, \\
K_2 = Z + \dfrac{\tau}{6}\Big[\sqrt{3}f(K_1) + 3f(K_2)\Big]\,.
\end{cases} \tag{21}$$

This Runge-Kutta scheme is of 3rd order but non-symplectic for standard Hamiltonian systems.

Scheme 3 (S3): fourth order scheme

$$\begin{cases}
\widetilde{Z} = Z + \dfrac{\tau}{2}[f(K_1) + f(K_2)]\,, \\
K_1 = Z + \dfrac{\tau}{12}\Big[3f(K_1) - (3-2\sqrt{3})f(K_2)\Big]\,, \\
K_2 = Z + \dfrac{\tau}{12}\Big[(3+2\sqrt{3})f(K_1) + 3f(K_2)\Big]\,.
\end{cases} \tag{22}$$

This Runge-Kutta scheme is of 4th order, revertible in τ, and symplectic for standard Hamiltonian systems ($f = J^{-1}\nabla H$).

6 Numerical Experiments

In this section, we will present the numerical simulation results performed in order to test the accuracy of the symplectic schemes and their conservativity of invariants or approximations in comparison with the nonsymplectic scheme, and show the differences between the numerical results of a same symplectic scheme applied to different standardized Hamiltonians.

The following initial conditions are used.

Condition 1. One-Soliton Solution

$$W(x,0) = 2\eta\sqrt{\frac{2}{a}}e^{2\chi xi}\mathrm{sech}[2\eta(x-x_1)]\,. \tag{23}$$

Condition 2. Two-Soliton Solution

$$W(x,0) = 2\eta_1\sqrt{\frac{2}{a}}e^{2\chi_1 xi}\mathrm{sech}[2\eta_1(x-x_a)] + 2\eta_2\sqrt{\frac{2}{a}}e^{2\chi_2 xi}\mathrm{sech}[2\eta_2(x-x_b)]\,. \tag{24}$$

Condition 3. Three-Soliton Solution

$$W(x,0) = \mathrm{sech}[x-x_3]\,. \tag{25}$$

Unless the contrary is stated the standard value for the nonlinear constant is $a = 2.0$.

We will apply the symplectic methods **S1, S3** to (9) with Hamiltonian functions (13), (16) or (19), and the non-symplectic scheme **S2** to (4).

In the following, we will call $err(A)(t) = A(t) - A(0)$ for any variable A.

Initial data (23) is the usual 1-soliton solution which is integrated without problems by many numerical methods. We present here the results of an integration with $\eta = 0.5, \chi = 0.5, x_1 = 0.0$ over the spatial interval $x \in [-750, 750]$ and temporal intervals $0 \le t \le 100$ for symplectic and non-symplectic method, with same integration parameters:

$$h = 0.3, \quad \tau = 0.02.$$

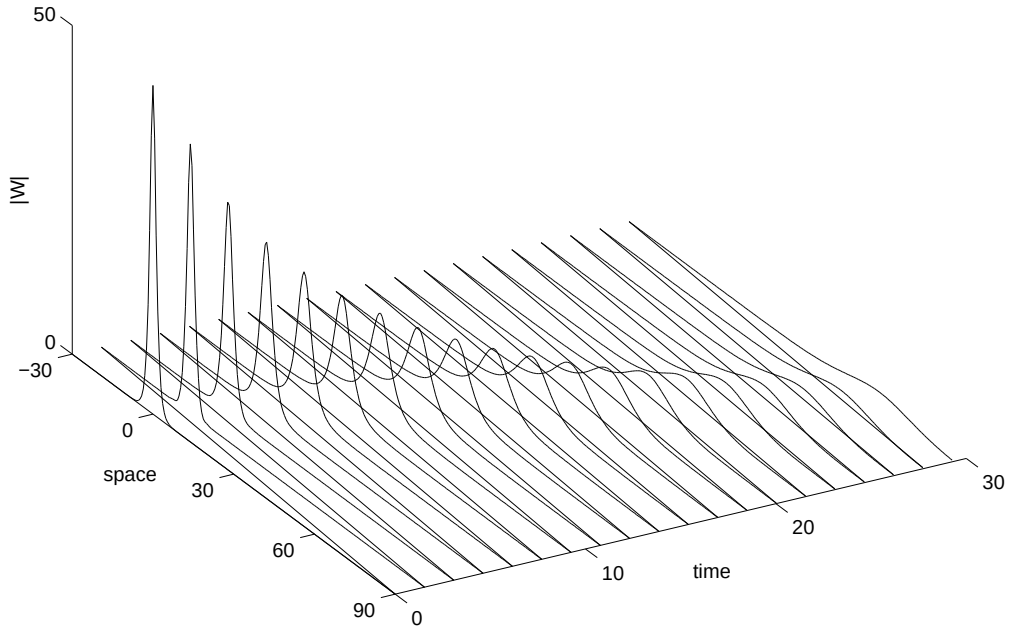

Fig. 1: single soliton motion computed by using scheme S2 to (4)

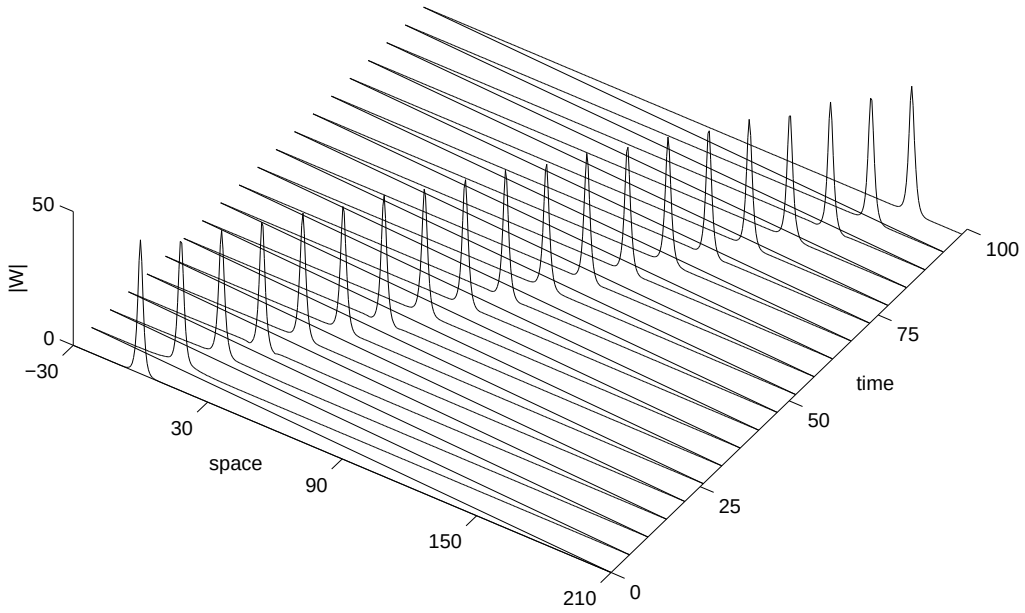

Fig. 2: single soliton motion computed by using scheme S1 to (9) with (13)

From Fig. 1 and Fig. 2 we find that the symplectic scheme can simulate the single soliton motion successfully, and the non-symplectic method cannot do even in a shorter interval $0 \leq t \leq 30$.

The expression in (24) is an initial data for a pair of solitons with different amplitudes and velocities and it is appropriate for the simulation of soliton collision (assuming that the soliton centers are initially set far away from each other). We have studied the following set of parameters $\eta_1 = \eta_2 = 0.5, \chi_1 = 0.25, \chi_2 = 0.025, x_a = 30.0, x_b = 0.0$ and

$$h = 0.3, \quad \tau = 0.02.$$

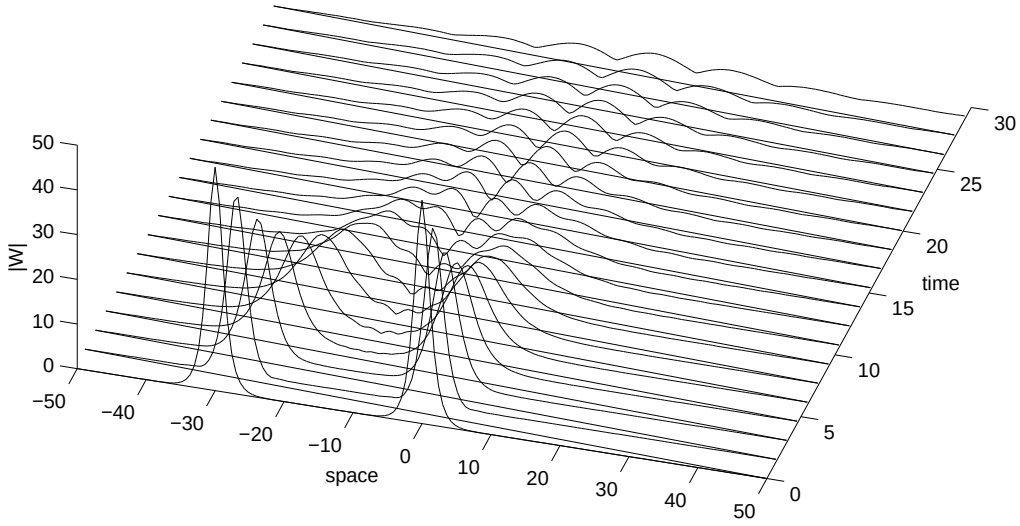

Fig. 3: propagation of two solitons computed by using scheme S2 to (4)

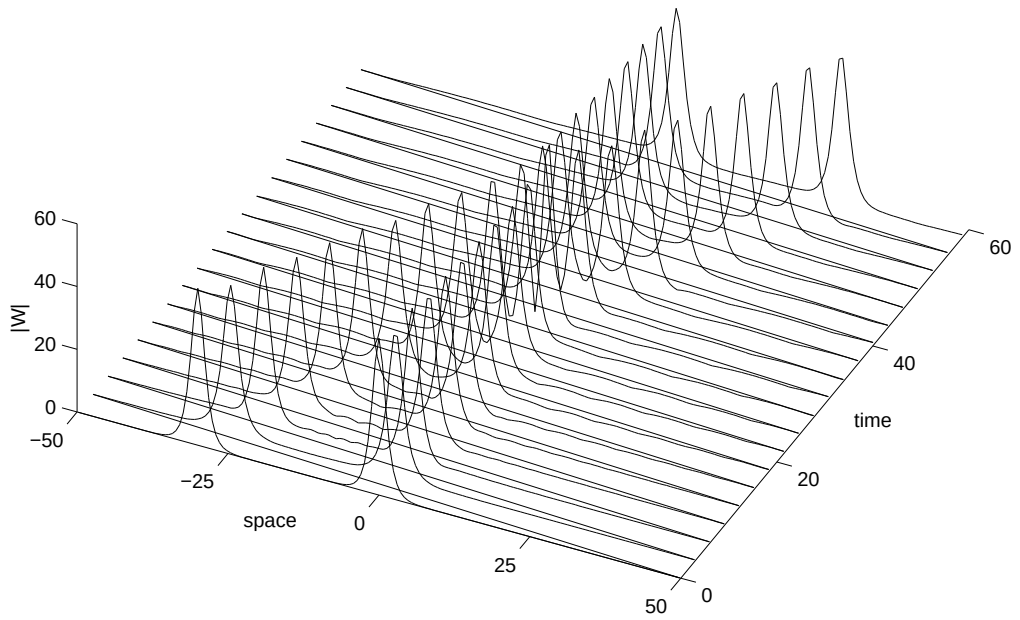

Fig. 4: propagation of two solitons computed by using scheme S1 to (9) with (13)

Fig. 3 and Fig. 4 show again the advantage of symplectic methods in preserving the motions of two solitons.

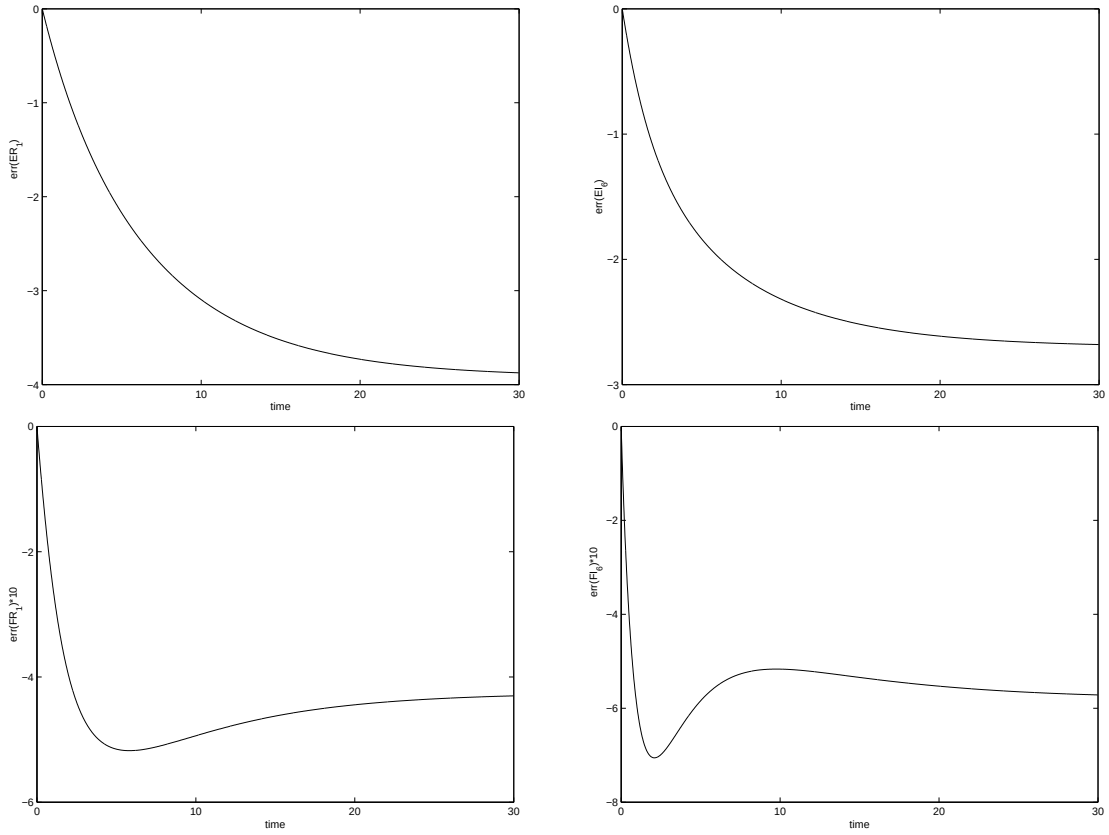

Fig. 5: evolution of ER_1, EI_6, FR_1 and FI_6 obtained by using scheme S2 to (4)

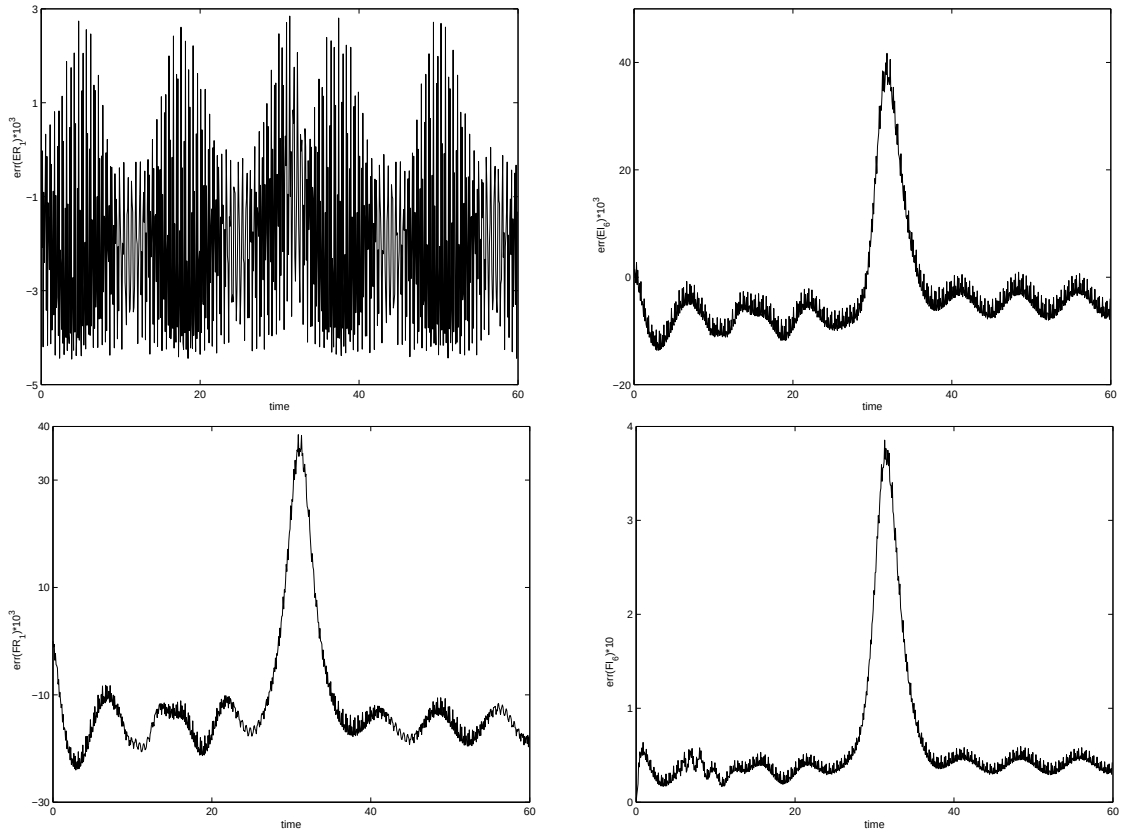

Fig. 6: evolution of ER_1, EI_6, FR_1 and FI_6 obtained by using scheme S1 to (9) with (13)

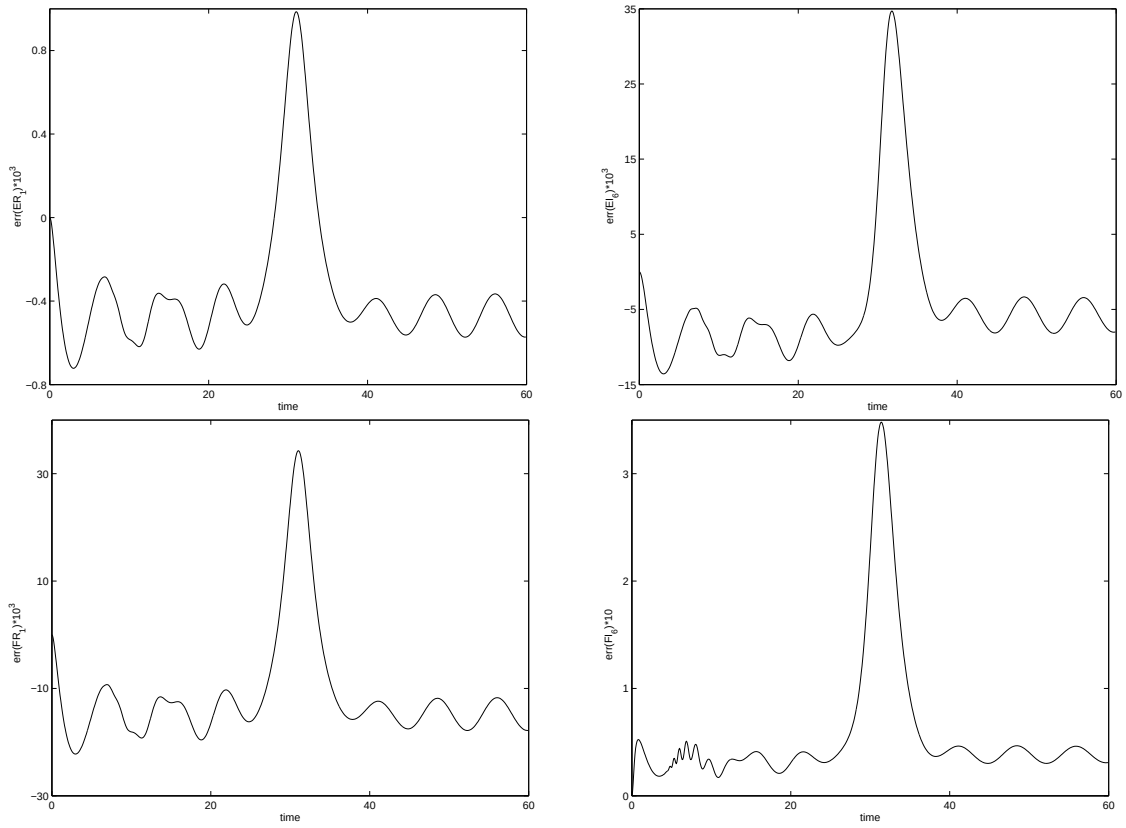

Fig. 7: evolution of ER_1, EI_6, FR_1 and FI_6 obtained by using scheme S1 to (9) with (16)

Since the evolution of other ER_j, EI_k, FR_l and FI_m is very similar, we plot only $err(ER_1)$, $err(EI_6)$, $err(FR_1)$ and $err(FI_6)$ in Fig. 5-7 respectively. Fig. 6-7 show that the numerical results for the invariants of the **A-L model** and the approximations to the conserved quantities of the original **NLSE** obtained by using symplectic scheme **S1** always undulate in small neighborhoods of the standard values respectively, while Fig. 5 shows that the corresponding numerical results obtained by using non-symplectic scheme **S2** degenerate with time. These phenomena are in good agreement with the solitons motion plotted in Fig. 3-4 respectively.

Though the behavior of invariants and approximations presented in both Fig. 6 and Fig. 7 is qualitatively good, one still easily finds the difference between these two figures. The plots in Fig. 7 seem to be much more "clean" than those in Fig. 6. In this sense one may say that it is the symmetry of Darboux transformation **II** (for simplicity, **D-T II**) that improves the computation results obtained by using Darboux transformation **I** (for simplicity, **D-T I**). On the other hand, We must point out that the implementation procedure for **D-T II** is much more complicated than that for **D-T I**. The following **Tables 1-4** show the comparative records of the implementation behavior for the 2-order symplectic scheme **S1** and the 4th-order symplectic scheme **S3** to integrate the Hamiltonian systems (9) given by (13) and by (16) respectively. We program in Fortran, solve the relevant equations by using simple iteration with double precision for computation. An error bound ϵ_0=1.0E−11 and a temporal interval for simulation $[0, 60]$ are fixed. Choosing a temporal step-size

τ and a maximum of iterative times N, one can compute the values of Y step by step: $Y(0) \to Y(\tau) \to Y(2\tau) \to Y(3\tau) \to \cdots$. For any j $(0 \le j \le 60/\tau - 1)$, iteration has to be used for $Y(j\tau) \to Y((j+1)\tau)$. This step transition process can be described as $Y(j\tau) = Y^{(1)} \to Y^{(2)} \to \cdots \to Y^{(l)} \to Y^{(l+1)} \to \cdots \to Y^{(N_j+1)} \approx Y((j+1)\tau)$. The iteration error of the l-th iterative step is counted by: $\epsilon^{(l)} = |Y^{(l+1)} - Y^{(l)}| = \sum_{i=-n}^{n} \Big(|u_i^{(l+1)} - u_i^{(l)}| + |v_i^{(l+1)} - v_i^{(l)}| \Big)$. If $N_j = N$ and $\epsilon^{(N)} > \epsilon_0$, then we note j and $\epsilon^{(N)}$. Choosing $\tau = 0.02$, $N = 48$, using scheme **S1** to (9) with (13) and with (16), we found that there are 6 and 1424 temporal points (among the total $60/0.02 = 3000$ steps) with iteration error greater than ϵ_0, and with maximum iteration error 9.5E−9 and 1.5E−7, respectively; when we enlarge the value of N to 96 or 396, these two indices are not changed for **S1** to integrate(9) with (13), but not stable and not improved for **S1** to integrate (9) with (16) (see **Table 1**). If we fix $N = 48$, and decrease the value of τ to 0.01, 0.002 and 0.001, then for **S1** to integrate (9) with (13), the number of the points with iteration error greater than ϵ_0 is fairly stable, and the maximum iteration error is regularly decreased with τ; and for **S1** to integrate (9) with (16), these two indices are not stable and not evidently improved (see **Table 2**). The case for scheme **S3** to integrate (9) with (13) or (16) is very similar to that for scheme **S1** (see **Table 3-4**).

Table 1: iteration errors for scheme S1 to integrate (9) with (13) and with (16) for 2-soliton motion, same temporal step-size, different maxima of iterative times

	$\tau = 0.02, N = 48$	$\tau = 0.02, N = 96$	$\tau = 0.02, N = 396$
D-T I	6, maxerr=9.5E−9	6, maxerr=9.5E−9	6, maxerr=9.5E−9
D-T II	1424, maxerr=1.5E−7	2198, maxerr=1.6E−7	1860, maxerr=1.9E−7

Table 2: iteration errors for scheme S1 to integrate (9) with (13) and (16) for 2-soliton motion, same maximum of iterative times, different temporal step-sizes

	$\tau = 0.01, N = 48$	$\tau = 0.002, N = 48$	$\tau = 0.001, N = 48$
D-T I	5, maxerr=4.3E−9	5, maxerr=7.8E−10	6, maxerr=4.3E−10
D-T II	928, maxerr=9.7E−7	1454, maxerr=4.4E−7	844, maxerr=1.6E−7

Table 3: iteration errors for scheme S3 to integrate (9) with (13) and (16) for 2-soliton motion, same temporal step-size, different maxima of iterative times

	$\tau = 0.02, N = 48$	$\tau = 0.02, N = 96$	$\tau = 0.02, N = 396$
D-T I	8, maxerr=9.9E−9	8, maxerr=9.9E−9	8, maxerr=9.9E−9
D-T II	1330, maxerr=3.7E−7	1352, maxerr=7.9E−7	1268, maxerr=1.0E−6

Table 4: iteration errors for scheme S3 to integrate (9) with (13) and (16) for 2-soliton motion, same maximum of iterative times, different temporal step-sizes

	$\tau = 0.01, N = 48$	$\tau = 0.002, N = 48$	$\tau = 0.001, N = 48$
D-T I	12, maxerr=3.0E−9	7, maxerr=5.9E−10	7, maxerr=3.1E−10
D-T II	1249, maxerr=9.0E−7	629, maxerr=2.5E−7	370, maxerr=2.1E−7

Tables 1-4 tell us that the Hamiltonian system (9) given by (13) is well-conditioned (except at a few temporal points) and has better solvability than that given by (16). So it would be safe to use **D-T I**. For symplectic computation of the Hamiltonian system (9) given by (16), it's also found that in the total temporal interval for simulation there are many points with iteration errors greater than ϵ_0, but only a few of them around the "maxerr" value. These errors even though added up are not enough essentially influential on the final numerical results. It still plays very well due to the symmetry. Nevertheless, one should be careful to use **D-T II**, especially for more complicated cases of motion.

Numerical experiments show that the Hamiltonian system (9) given by (19) is not numerically integrable by the symplectic scheme **S1** or **S3**. Running of the Fortran program can last only several temporal steps no matter how small the step-size is chosen, because of the appearance of "DOMAIN error in sqrt".

Numerical experiments show that the numerical results obtained by using the non-symplectic scheme **S2** to the Hamiltonian system (9) given by (13) or by (16) are very similar to those obtained by using **S2** directly to (4). And obviously the simulation process of the former is more time-consuming than that of the latter.

Finally, we have used the initial data (25), which is usually considered to be a more difficult "quality" test for numerical schemes because of the appearance of large spatial and temporal gradients in the solution. For $a = 2N^2 (N = 2, 3, \cdots)$ Miles has shown that (25) corresponds to a bounded state of N solitons [11]. For the case $a = 18$, we found that for $h \leq 0.06667$, with some proper temporal stepsize which makes simple iteration practicable, the 2nd-order symplectic scheme **S1** represents accurately the solution without problems (Fig. 9 where $x_3 = 0.0$). This is a very good result and provides convergence to the correct solution with a relatively rough spatial grid, while the 3rd-order non-symplectic scheme **S2** studied for comparison fails to do so (Fig. 8).

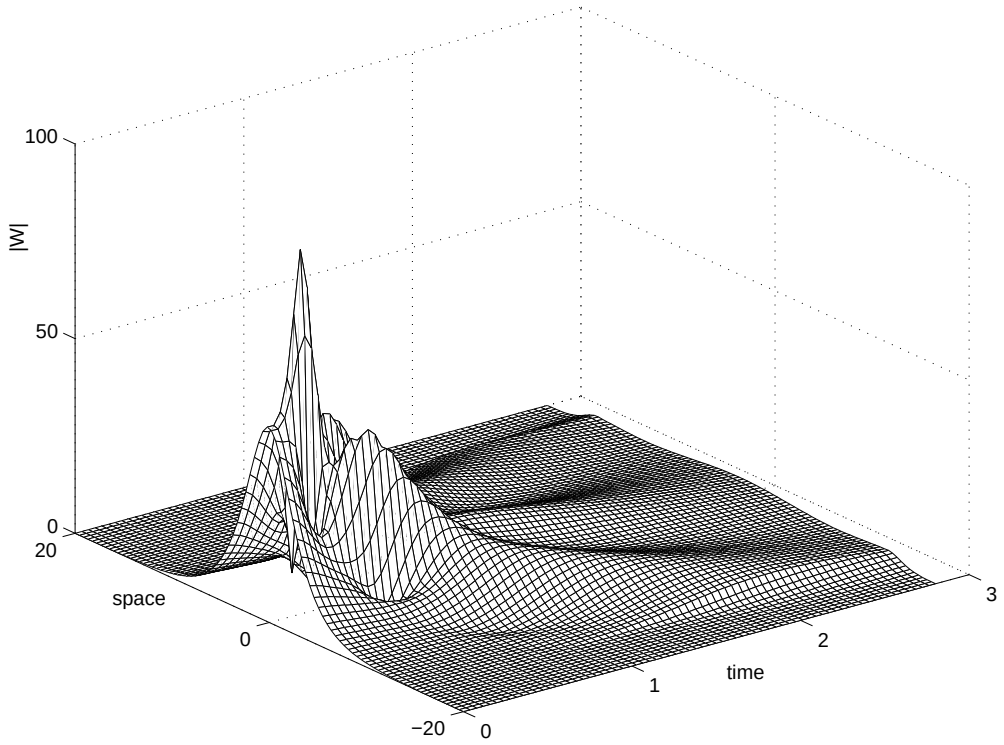

Fig. 8: propagation of three-soliton bounded state computed by using scheme S2 to (4)

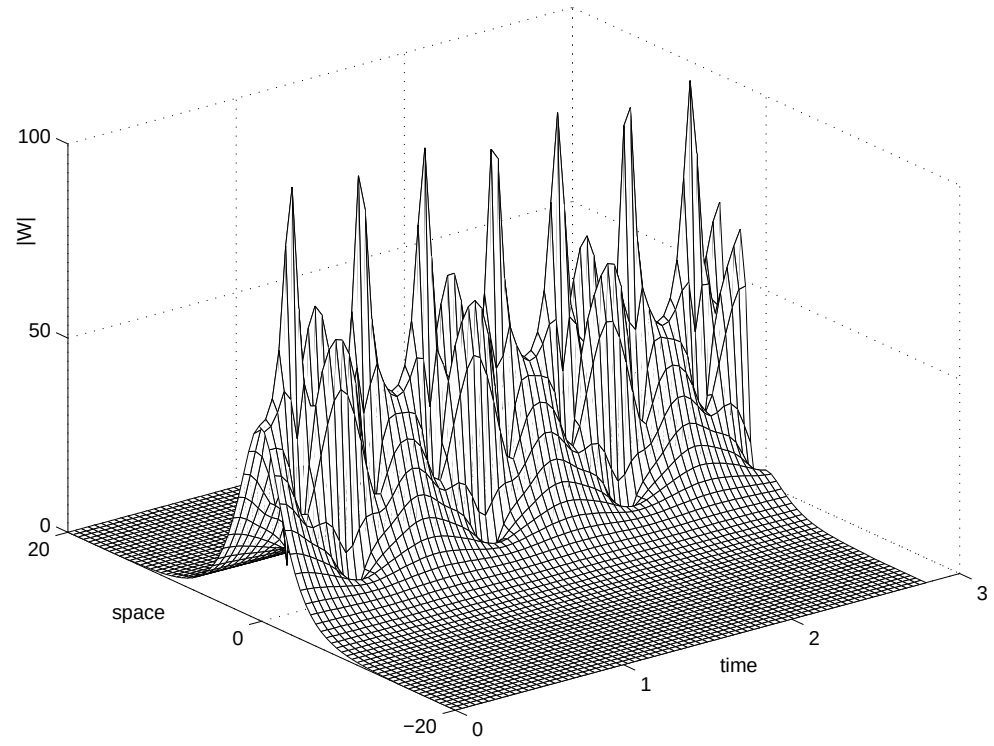

Fig. 9: propagation of three-soliton bounded state computed by using scheme S1 to (9) with (13)

7 Concluding Remarks

The Ablowitz-Ladik model of the Nonlinear Schrödinger Equation is a completely integrable general Hamiltonian system which can be standardized via Darboux transformation. When suitable Darboux transformation is chosen, the symplectic methods applied to the standardized Hamiltonian system (especially obtained via symmetric Darboux transformations) have overwhelming superiorities over the non-symplectic scheme applied directly to the A-L model, such as long-term tracking of solitons motion, long-term preserving of discrete invariants of the **A-L model** and also the conserved quantities of the original **NLSE** up to a very samll error.

On the other hand, the main disadvantage of this method (Ablowitz-Ladik+Darboux transformation+symplectic integration, simply, **ALDTSI**) is that due to the complexity of the standardized Hamiltonian, we have to use iterative methods to solve the highly nonlinear system. This fact makes the implementation process difficult when the system is ill-conditioned at some temporal points even though symmetry is considered for the choice of Darboux transformation, and the implementation time consuming when compared with spectral methods [14] or linearly implicit finite difference schemes [18] which are commonly used to integrate the **NLSE**. So it is also most important to choose a suitable Darboux transformation in our procedure. When noncritical problems are considered, it is a thing to choose a scheme; but for more difficult or complicated problems, the additional guaranties provided by **ALDTSI** maybe of high interest, and in any case this method provides a safe way to check the results of the faster but less accurate methods when simple physical problems are to be studied.

References

[1] M.J. Ablowitz & J.F. Ladik, Nonlinear differential-difference equations and Fourier Analysis, *J. Math. Phys.* **17**(6), 1011-1018 (1976).

[2] R.E. Abraham & J.E. Marsden, *Foundations of Mechanics*, Benjamin-Cummings, Reading, MA, (1978).

[3] V.I. Arnold, *Mathematical Methods of Classical Mechanics*, Springer, New York, (1978).

[4] P.J. Channell and J.C. Scovel, Symplectic Integration of Hamiltonian Systems, *Nonlinearity* **3**(2), 231-259 (1990).

[5] R.K. Dodd, J.C. Eibeck, J.D. Gibbon & H.C. Morris, *Solitons and Nonlinear Wave Equation*, Academic Press, (1982).

[6] K. Feng, On Difference Schemes and Symplectic Geometry, In *Proceedings of the 1984 Beijing Symposium on Differential Geometry and Differential Equations*, Edited by K. Feng, Beijing: Science Press, 42-58 (1985).

[7] E. Hairer, Ch. Lubich, G. Wanner, *Geometric Numerical Integration*, Springer, (2002).

[8] A. Hasegawa, *Optical Solitons in Fibers*, Springer-Verlag, (1989).

[9] B.M. Herbst, F. Varadi & M.J. Ablowitz, Symplectic Methods for the Nonlinear Schrödinger Equation, *Math. Comput. Simul.*, **37**, 353-369 (1994).

[10] V.V. Konotop & L. Vázquez, *Nonlinear Random Waves*, World Scientific, Singapore (1994).

[11] J.W. Miles, An envelope soliton problem, *SIAM J. Appl. Math.* **41**(2) 227-230 (1981).

[12] J.M. Sanz-Serna & M.P. Calvo, *Numerical Hamiltonian problems*, Chapman & Hall, London, (1994).

[13] C.M. Schober, Symplectic Integrators for the Ablowitz-Ladik Discrete Nonlinear Schrödinger Equation, *Phys. Lett. A* **259**, 140-151 (1999).

[14] T.R. Taha and M. Ablowitz, Analytical and Numerical Aspects of Certain Nonlinear Evolution Equations. II. Numerical, Nonlinear Schrödinger Equation, *J. Computa. Phys.* **55**(2) 203-230 (1984).

[15] Y.F. Tang, V.M. Pérez-García & L. Vázquez, Symplectic Methods for the Ablowitz-Ladik Model, *Appli. Math. Comput.* **82**, 17-38 (1997).

[16] Y.F. Tang, Standardization of the Ablowitz-Ladik Model as a Hamiltonian System, *Research Reprot 1997-006 of ICMSEC, CAS*, (1997). Unpublished.

[17] V.E. Zakharov & A.B. Shabat, Interaction Between Solitions in a Stable Medium, *Sov. Phys.-JETP* **37**(5), 823-828 (1973).

[18] F. Zhang, V.M. Pérez-García and L. Vázquez, Numerical Simulation of Nonlinear Schrödionger Systems: A New Conservative Scheme, *Appl. Math. Comput.* **71**(2-3) 165-177 (1995).

Appendix

Through straightforward but tedious calculation, we get discrete invariants of A-L model (2), the first 6 are given as follows:

$$
\begin{aligned}
S_1 &= \sum_k W_{k+1}\overline{W}_k,\\
S_2 &= \frac{ah^2}{4}\sum_k W_{k+1}^2\overline{W}_k^2+\sum_k W_{k+1}\overline{W}_{k-1}U_k,\\
S_3 &= \frac{a^2h^4}{12}\sum_k W_{k+1}^3\overline{W}_k^3+\frac{ah^2}{2}\sum_k W_{k+1}^2\overline{W}_k\overline{W}_{k-1}U_k+\frac{ah^2}{2}\sum_k W_{k+1}W_k\overline{W}_{k-1}^2U_k+\sum_k W_{k+1}\overline{W}_{k-2}U_kU_{k-1},\\
S_4 &= \frac{a^3h^6}{32}\sum_k W_{k+1}^4\overline{W}_k^4+\frac{a^2h^4}{4}\sum_k W_{k+1}^3\overline{W}_k^2\overline{W}_{k-1}U_k+\frac{a^2h^4}{4}\sum_k W_{k+1}^2|W_k|^2\overline{W}_{k-1}^2U_k\\
&\quad+\frac{ah^2}{2}\sum_k W_{k+1}^2\overline{W}_k\overline{W}_{k-2}U_kU_{k-1}+\frac{ah^2}{4}\sum_k W_{k+1}^2\overline{W}_{k-1}^2U_k^2+\frac{a^2h^4}{4}\sum_k W_{k+1}W_k^2\overline{W}_{k-1}^3U_k\\
&\quad+ah^2\sum_k W_{k+1}W_k\overline{W}_{k-1}\overline{W}_{k-2}U_kU_{k-1}+\frac{ah^2}{2}\sum_k W_{k+1}W_{k-1}\overline{W}_{k-2}^2U_kU_{k-1}\\
&\quad+\sum_k W_{k+1}\overline{W}_{k-3}U_kU_{k-1}U_{k-2},\\
S_5 &= \frac{a^4h^8}{80}\sum_k W_{k+1}^5\overline{W}_k^5+\frac{a^3h^6}{8}\sum_k W_{k+1}^4\overline{W}_k^3\overline{W}_{k-1}U_k+\frac{a^3h^6}{8}\sum_k W_{k+1}^3|W_k|^2\overline{W}_k\overline{W}_{k-1}^2U_k\\
&\quad+\frac{a^2h^4}{4}\sum_k W_{k+1}^3\overline{W}_k^2\overline{W}_{k-2}U_kU_{k-1}+\frac{a^2h^4}{4}\sum_k W_{k+1}^3\overline{W}_k\overline{W}_{k-1}^2U_k^2+\frac{a^3h^6}{8}\sum_k W_{k+1}^2W_k|W_k|^2\overline{W}_{k-1}^3U_k\\
&\quad+\frac{a^2h^4}{2}\sum_k W_{k+1}^2|W_k|^2\overline{W}_{k-1}\overline{W}_{k-2}U_kU_{k-1}+\frac{a^2h^4}{4}\sum_k W_{k+1}^2W_k\overline{W}_{k-1}^3U_k^2\\
&\quad+\frac{a^2h^4}{4}\sum_k W_{k+1}^2W_{k-1}\overline{W}_k\overline{W}_{k-2}^2U_kU_{k-1}+\frac{ah^2}{2}\sum_k W_{k+1}^2\overline{W}_k\overline{W}_{k-3}U_kU_{k-1}U_{k-2}\\
&\quad+\frac{ah^2}{2}\sum_k W_{k+1}^2\overline{W}_{k-1}\overline{W}_{k-2}U_k^2U_{k-1}+\frac{a^3h^6}{8}\sum_k W_{k+1}W_k^3\overline{W}_{k-1}^4U_k\\
&\quad+\frac{3a^2h^4}{4}\sum_k W_{k+1}W_k^2\overline{W}_{k-1}^2\overline{W}_{k-2}U_kU_{k-1}+\frac{a^2h^4}{2}\sum_k W_{k+1}W_k|W_{k-1}|^2\overline{W}_{k-2}^2U_kU_{k-1}\\
&\quad+ah^2\sum_k W_{k+1}W_k\overline{W}_{k-1}\overline{W}_{k-3}U_kU_{k-1}U_{k-2}+\frac{ah^2}{2}\sum_k W_{k+1}W_k\overline{W}_{k-2}^2U_kU_{k-1}^2\\
&\quad+\frac{a^2h^4}{4}\sum_k W_{k+1}W_{k-1}^2\overline{W}_{k-2}^3U_kU_{k-1}+ah^2\sum_k W_{k+1}W_{k-1}\overline{W}_{k-2}\overline{W}_{k-3}U_kU_{k-1}U_{k-2}\\
&\quad+\frac{ah^2}{2}\sum_k W_{k+1}W_{k-2}\overline{W}_{k-3}^2U_kU_{k-1}U_{k-2}+\sum_k W_{k+1}\overline{W}_{k-4}U_kU_{k-1}U_{k-2}U_{k-3},\\
S_6 &= \frac{a^5h^{10}}{192}\sum_k W_{k+1}^6\overline{W}_k^6+\frac{a^4h^8}{16}\sum_k W_{k+1}^5\overline{W}_k^4\overline{W}_{k-1}U_k+\frac{a^4h^8}{16}\sum_k W_{k+1}^4|W_k|^2\overline{W}_k^2\overline{W}_{k-1}^2U_k\\
&\quad+\frac{a^3h^6}{8}\sum_k W_{k+1}^4\overline{W}_k^3\overline{W}_{k-2}U_kU_{k-1}+\frac{3a^3h^6}{16}\sum_k W_{k+1}^4\overline{W}_k^2\overline{W}_{k-1}^2U_k^2+\frac{a^4h^8}{16}\sum_k W_{k+1}^3|W_k|^4\overline{W}_{k-1}^3U_k\\
&\quad+\frac{a^3h^6}{4}\sum_k W_{k+1}^3|W_k|^2\overline{W}_k\overline{W}_{k-1}\overline{W}_{k-2}U_kU_{k-1}+\frac{a^3h^6}{4}\sum_k W_{k+1}^3|W_k|^2\overline{W}_{k-1}^3U_k^2\\
&\quad+\frac{a^3h^6}{8}\sum_k W_{k+1}^3W_{k-1}\overline{W}_k^2\overline{W}_{k-2}^2U_kU_{k-1}+\frac{a^2h^4}{4}\sum_k W_{k+1}^3\overline{W}_k^2\overline{W}_{k-3}U_kU_{k-1}U_{k-2}\\
&\quad+\frac{a^2h^4}{2}\sum_k W_{k+1}^3\overline{W}_k\overline{W}_{k-1}\overline{W}_{k-2}U_k^2U_{k-1}+\frac{a^2h^4}{12}\sum_k W_{k+1}^3\overline{W}_{k-1}^3U_k^3+\frac{a^4h^8}{16}\sum_k W_{k+1}^2W_k^2|W_k|^2\overline{W}_{k-1}^4U_k\\
&\quad+\frac{3a^3h^6}{8}\sum_k W_{k+1}^2W_k|W_k|^2\overline{W}_{k-1}^2\overline{W}_{k-2}U_kU_{k-1}+\frac{3a^3h^6}{16}\sum_k W_{k+1}^2W_k^2\overline{W}_{k-1}^4U_k^2\\
&\quad+\frac{a^3h^6}{4}\sum_k W_{k+1}^2|W_k|^2|W_{k-1}|^2\overline{W}_{k-2}^2U_kU_{k-1}+\frac{a^2h^4}{2}\sum_k W_{k+1}^2|W_k|^2\overline{W}_{k-1}\overline{W}_{k-3}U_kU_{k-1}U_{k-2}
\end{aligned}
$$

$$+\frac{a^2h^4}{4}\sum_k W_{k+1}^2|W_k|^2\overline{W}_{k-2}^2U_kU_{k-1}^2+\frac{3a^2h^4}{4}\sum_k W_{k+1}^2W_k\overline{W}_{k-1}^2\overline{W}_{k-2}U_k^2U_{k-1}$$

$$+\frac{a^3h^6}{8}\sum_k W_{k+1}^2W_{k-1}^2\overline{W}_k\overline{W}_{k-2}^3U_kU_{k-1}+\frac{a^2h^4}{2}\sum_k W_{k+1}^2W_{k-1}\overline{W}_k\overline{W}_{k-2}\overline{W}_{k-3}U_kU_{k-1}U_{k-2}$$

$$+\frac{a^2h^4}{4}\sum_k W_{k+1}^2|W_{k-1}|^2\overline{W}_{k-2}^2U_k^2U_{k-1}+\frac{a^2h^4}{4}\sum_k W_{k+1}^2W_{k-2}\overline{W}_k\overline{W}_{k-3}^2U_kU_{k-1}U_{k-2}$$

$$+\frac{ah^2}{2}\sum_k W_{k+1}^2\overline{W}_k\overline{W}_{k-4}U_kU_{k-1}U_{k-2}U_{k-3}+\frac{ah^2}{2}\sum_k W_{k+1}^2\overline{W}_{k-1}\overline{W}_{k-3}U_k^2U_{k-1}U_{k-2}$$

$$+\frac{ah^2}{4}\sum_k W_{k+1}^2\overline{W}_{k-2}^2U_k^2U_{k-1}^2+\frac{a^4h^8}{16}\sum_k W_{k+1}W_k^4\overline{W}_{k-1}^5U_k+\frac{a^3h^6}{2}\sum_k W_{k+1}W_k^3\overline{W}_{k-1}^3\overline{W}_{k-2}U_kU_{k-1}$$

$$+\frac{3a^3h^6}{8}\sum_k W_{k+1}W_k^2\left|W_{k-1}\right|^2\overline{W}_{k-1}\overline{W}_{k-2}^2U_kU_{k-1}+\frac{3a^2h^4}{4}\sum_k W_{k+1}W_k^2\overline{W}_{k-1}^2\overline{W}_{k-3}U_kU_{k-1}U_{k-2}$$

$$+\frac{3a^2h^4}{4}\sum_k W_{k+1}W_k^2\overline{W}_{k-1}\overline{W}_{k-2}^2U_kU_{k-1}^2+\frac{a^3h^6}{4}\sum_k W_{k+1}W_kW_{k-1}\left|W_{k-1}\right|^2\overline{W}_{k-2}^3U_kU_{k-1}$$

$$+a^2h^4\sum_k W_{k+1}W_k|W_{k-1}|^2\overline{W}_{k-2}\overline{W}_{k-3}U_kU_{k-1}U_{k-2}+\frac{a^2h^4}{2}\sum_k W_{k+1}W_kW_{k-1}\overline{W}_{k-2}^3U_kU_{k-1}^2$$

$$+\frac{a^2h^4}{2}\sum_k W_{k+1}W_kW_{k-2}\overline{W}_{k-1}\overline{W}_{k-3}^2U_kU_{k-1}U_{k-2}+ah^2\sum_k W_{k+1}W_k\overline{W}_{k-2}\overline{W}_{k-3}U_kU_{k-1}^2U_{k-2}$$

$$+ah^2\sum_k W_{k+1}W_k\overline{W}_{k-1}\overline{W}_{k-4}U_kU_{k-1}U_{k-2}U_{k-3}+\frac{a^3h^6}{8}\sum_k W_{k+1}W_{k-1}^3\overline{W}_{k-2}^4U_kU_{k-1}$$

$$+\frac{3a^2h^4}{4}\sum_k W_{k+1}W_{k-1}^2\overline{W}_{k-2}^2\overline{W}_{k-3}U_kU_{k-1}U_{k-2}+\frac{a^2h^4}{2}\sum_k W_{k+1}W_{k-1}|W_{k-2}|^2\overline{W}_{k-3}^2U_kU_{k-1}U_{k-2}$$

$$+ah^2\sum_k W_{k+1}W_{k-1}\overline{W}_{k-2}\overline{W}_{k-4}U_kU_{k-1}U_{k-2}U_{k-3}+\frac{ah^2}{2}\sum_k W_{k+1}W_{k-1}\overline{W}_{k-3}^2U_kU_{k-1}U_{k-2}^2$$

$$+\frac{a^2h^4}{4}\sum_k W_{k+1}W_{k-2}^2\overline{W}_{k-3}^3U_kU_{k-1}U_{k-2}+ah^2\sum_k W_{k+1}W_{k-2}\overline{W}_{k-3}\overline{W}_{k-4}U_kU_{k-1}U_{k-2}U_{k-3}$$

$$+\frac{ah^2}{2}\sum_k W_{k+1}W_{k-3}\overline{W}_{k-4}^2U_kU_{k-1}U_{k-2}U_{k-3}+\sum_k W_{k+1}\overline{W}_{k-5}U_kU_{k-1}U_{k-2}U_{k-3}U_{k-4}$$

where $U_k=1+\frac{ah^2}{2}\left|W_k\right|^2$.